An Angle-Based Bi-Objective Optimization Algorithm for Redundancy Allocation in Presence of Interval Uncertainty

Yue Xu, Dechang Pi, Shengxiang Yang, *Senior Member, IEEE*, Yang Chen, Shuo Qin, and Enrico Zio, *Senior Member, IEEE*

***Abstract*— Uncertainty is a practical issue in system design optimization because some characteristics of components, such as reliability and cost, cannot be determined precisely in many situations. Considering the imprecise characteristics of components, few works have focused on the multi-objective optimization for the redundancy allocation due to the challenges of comparing multi intervals. To tackle the issue, a novel angle-based bi-objective redundancy allocation algorithm is proposed in this study, introducing three original contributions: 1) An angle-based interval crowding distance (ICA) is especially designed for effective performance and reduced computational time; 2) Two techniques are applied to tackle the problem: An elite selection for mutation is presented for generating better offsprings; A penalty-guided constraint handling technique is introduced for converting the problem into an unconstrained one. 3) Since a set of optimal solutions is obtained by the proposed method and no preference on uncertainties is provided, this paper proposes a novel knee interval method to help DMs make a decision. To be specific, the proposed ICA can describe the distribution of the whole population intuitively and effectively, considering not only the angle between two compared individuals but also the angle range of the interval values. The computational results from two typical experiments demonstrate that the proposed algorithm is more efficient than other state-of-the-art algorithms, generating Pareto sets with less repeating individuals, stronger convergence, wider distribution, less imprecision, and reduced computational time.**

Manuscript received 25 August 2021; revised 27 October 2021 and 3 January 2022; accepted 26 January 2022. Date of publication 16 February 2022; date of current version 6 January 2023. This article was recommended for publication by Associate Editor V. Augusto and Editor Q. Zhao upon evaluation of the reviewers' comments. This work was supported in part by the National Science and Technology Innovation 2030-Key Project of "New Generation Artificial Intelligence" under Grant 2021ZD0113103, in part by the Postgraduate Research and Practice Innovation Program of Jiangsu Province under Grant KYCX19_0202, and in part by the China Scholarship Council under Grant 202006830131. *(Corresponding author: Dechang Pi.)*

Yue Xu, Dechang Pi, Yang Chen, and Shuo Qin are with the College of Computer Science and Technology and the College of Artificial Intelligence, Nanjing University of Aeronautics and Astronautics, Nanjing 210016, China (e-mail: ayue@nuaa.edu.cn; dc.pi@nuaa.edu.cn; shawn.cy@nuaa.edu.cn; qinshuo@nuaa.edu.cn).

Shengxiang Yang is with the School of Computer Science and Informatics, De Montfort University, Leicester LE1 9BH, U.K. (e-mail: syang@dmu.ac.uk).

Enrico Zio is with the Department of Energy, Centre for Research on Risk and Crises (CRC), Ecole de Mines, ParisTech, PSL University, 75006 Paris, France, and also with the Politecnico di Milano, 20133 Milan, Italy (e-mail: enrico.zio@mines-paristech.fr; enrico.zio@polimi.it).

Color versions of one or more figures in this article are available at https://doi.org/10.1109/TASE.2022.3148459.

Digital Object Identifier 10.1109/TASE.2022.3148459

***Note to Practitioners*— This article is motivated by two practical problems in multi-objective redundancy allocation in presence of interval uncertainty: First, this paper tries to solve the multi-objective redundancy allocation problem with the imprecise characteristics of components, which is rarely considered in the field of reliability optimization design. Second, the calculation of the crowding distance needs extra time cost and is less efficient. To tackle this issue, an interval crowding angle is especially designed, considering not only the angle between two compared individuals, but also the angle range of the interval values. The proposed method can be embedded in most multi-objective interval evolutionary algorithms to compute the diversity of the individuals. The goal of this study is to allocate the economy and high-reliable components for practitioners. The computational results verify its effectiveness and efficiency. Besides, in many cases the practitioners know only few or no preferences, this paper proposes a knee point analysis of interval values that allows practitioners to select the optimal solution with large hypervolume and less imprecision among a set of solutions.**

***Index Terms*— Redundancy allocation problem, interval uncertainty, multi-objective optimization, interval crowding angle, knee interval.**

I. Introduction

THE redundancy allocation problem (RAP) has been broadly investigated in system engineering. In a RAP, the number of redundant components and redundancy levels are allocated in each subsystem, with the goal of maximizing the system reliability and/or minimizing the system cost. Both single-objective optimization [1]–[5] and multi-objective optimization problems [6]–[11] have been considered in determined environments, assuming that the component characteristics are certain.

However, the characteristics of components are uncertain in practice [12]. For practical purposes, there are two types of uncertainties: aleatory and epistemic [13]. The former one is caused by the inherent randomness of the component behavior [14], also named stochastic uncertainty [15], irreducible uncertainty, or inherent uncertainty [16]. The latter is due to the imprecision of the model representation of the system behavior, in terms of the structural and parameter uncertainty [17]. For example, the reliability or cost of a component is difficult to determine as fixed values in many situations. As mentioned in [18], "the RAP is always deterministic with vague or imprecise statements, which can be boiled down to problems of observing the parameters themselves, deficiency in history and statistical data, insufficient theory,

incomplete knowledge and the subjectivity and preference of human judgment, etc."

From the perspective of decision makers (DMs), the approaches for uncertain optimization problems (UOPs) can be divided into three categories: *priori*, *interactive* and *posteriori* [19]. The difference between these approaches is when DMs provide their preferences: in advance, during the search, or at the end of the optimization process. There are various studies considering preference in uncertain multi-objective optimization problems, such as [20], [21], but it is difficult for DMs to offer their preferences when they know little or nothing about uncertainties. Furthermore, it is risky to make assumptions with insufficient information. Hence, this paper focuses on the *posteriori* methods: The optimization process is conducted without DMs' preferences, and a set of optimal solutions is provided for DMs to select the most preferred one according to their preferences [19]. If no preference is presented, this paper analyzes the knee interval to help DMs to make a decision. The optimization problem in an uncertain environment by *posteriori* methods can be modeled as stochastic programming [22], [23], fuzzy programming [24], [25], or interval programming [26]–[28]. Compared with the former two approaches, interval programming has the benefit of requiring no additional function information when formulating the problem, like, probability distributions in stochastic programming and membership functions in fuzzy programming [29]. Besides, the variables in the former two approaches can be converted to intervals by a cut set and a confidence level, respectively [30]. Therefore, interval programming is employed to tackle the RAP with interval-valued characteristics due to its simplicity and wide application. For example, a genetic algorithm (GA)-based penalty function technique was proposed by Gupta *et al.* to solve the constrained RAP with interval-valued reliabilities of components [31]. Feizollahi and Modarres developed a robust deviation framework (Min-Max regret approach) for the RAP with imprecise component reliability [26]. Then, Roy *et al.* presented an entropy-based region reducing GA for the reliability redundancy allocation problem, denoted as RRAP [27]. In practice, the multi-objective interval optimization is more meaningful but is also more challenging, since the comparison of interval values is relatively difficult. Considering this issue, Sahoo *et al.* converted the multi-objective RAP into a single one, with the Big-M penalty strategy, and utilized a GA for solving it [32]. Besides, a game-based solution selection was developed by Cao *et al.* for the multi-objective RAP [33], where entropy was selected as a metric for modeling the imprecision of interval-valued parameters.

The above studies have adopted some transformation method, without considering the interval dominance relationship, which will be further discussed in Section III. Taking the dominance of interval numbers into account, Zhang and Chen adapted the multi-objective particle swarm optimization (MOPSO) algorithm [28]. In their method, a new order relation of interval numbers was designed without extra knowledge about the underlying distribution or the preferences of decision makers; an extended crowding distance was also presented to produce well-distributed Pareto fronts.

Regarding the interval dominance relationship, this paper tries to further advance the state-of-the-art on the multi-objective interval RAP. The major contributions of this study are summarized as follows.

1) To the best of our knowledge, the angle-based technique is employed for the first time to deal with the interval optimization problem. An interval crowding angle is especially designed, considering not only the angle between two compared individuals, but also the angle range of the interval values. To be specific, this method is relatively simple with less parameters and can be widely employed in many practical applications for describing the population distribution;
2) Two effective techniques are applied to solve the RAPs in presence of interval uncertainty: (1) Elite selection for mutation keeps the top individuals with good rank and wide distribution in the population; (2) The constrained problem is transformed into an unconstrained one via the penalty function;
3) In this paper, the optimization process is conducted without extra knowledge about the DMs' preferences. Furthermore, a novel knee interval calculation method is presented in this paper, aiming at helping DMs to select the most promising solution among the Pareto Front, with larger hypervolume and less imprecision.

The rest of the paper is arranged as follows. The related work including the review of interval multi-objective optimization and angle-based multi-objective optimization is detailed in Section II. Furthermore, the motivation of this study is also presented in this section. Subsequently, the formulation of the multi-objective RAP with interval uncertainty is shown in Section III. In Section IV, a novel interval angle-based approach is proposed to solve the problem with interval crowding angle, elite selection for mutation and constraint handling. Experimental results and analysis are supplied in Section V. The paper is ended with conclusions and perspectives in Section VI.

II. Related Work and Motivation

The problem considered in this study is an interval multi-objective optimization problem (IMOP), considering more than one objective conflicting with each other, and at least one objective and (or) constraint is interval-valued. Without loss of generality, a constrained IMOP is formulated as follows.

$$\begin{aligned} &max f(x,c) = (f_1(x,c), f_2(x,c), \ldots, f_M(x,c))^T \\ &s.t.\ c = (c_1, c_2, \ldots, c_K)^T, \\ &\quad c_k = [c_{kL}, c_{kU}], \quad k = 1, 2, \ldots, K \\ &\quad g(x) = (g_1(x), g_2(x), \ldots, g_{n_g}(x))^T \leq 0 \\ &\quad h(x) = (h_1(x), h_2(x), \ldots, h_{n_h}(x))^T = 0 \end{aligned} \tag{1}$$

where x is the decision vector, $f_m(x,c), m = 1, 2, \ldots, M$, is the mth objective with interval parameters, c is a vector of interval-valued parameters, of which c_k is the kth component with c_{kL} and c_{kU} denoting the lower and upper bounds of c_k, respectively. Besides, g_i and h_j represent the ith inequality and jth equality constraints where $i = 1, 2, \ldots, n_g$, and $j = 1, 2, \ldots, n_h$, respectively.

A. Review of Interval Multi-Objective Optimization

Generally, the following two methods are taken into consideration for the IMOP. The first method is to convert the interval values into a deterministic one, as mentioned in [32], [33]. This method is relatively simple, not considering the relationship of interval dominance. Keeping this in mind, Cheng *et al.* firstly transformed an IMOP into a min-max optimization problem and, then, proposed a hierarchical algorithm composed of GA and a nonlinear programming approach to solve it [34]. A popular approach was presented by Jiang *et al.* to utilize the middle point and the width of an interval to convert the problem [35]. This method was later used in [36], [37] and verified to have good performance. Although the transformation method is easy to be understood and implemented, the converted problem is significantly different from the original one. As analyzed in [29], different transformation methods will bring out different deterministic problems for the same interval-value problem. For DMs, solutions obtained by these transformation methods can be ambiguous: as a consequence, it is difficult to find the optimal solution from different solution sets.

The other method is directly based on the interval dominance using evolutionary algorithms, which can avoid losing valuable information and adding redundant information, thus obtaining more precise solutions [29]. Along this line, Limbourg and Aponte proposed the concept of IMOPs for the first time and developed an interval multi-objective optimization algorithm, named imprecision-propagating multi-objective optimization algorithm (IP-MOEA, for short) [38]. In their study, a new interval dominance relation $>_{IN}$ and a hypervolume-based crowding distance (CD) were proposed for tackling the issue. However, the interval numbers were not compared when one enclosed the other in IP-MOEA.

Researches of interval dominance relation have become a trend in recent years, such as interval credibility [39], [40], interval probability dominant strategy [41], α-degree Pareto dominance [42], possibility degree [43]. In [44], a large amount of related interval programming methods have been reviewed, and an ensemble framework was designed for choosing a suitable approach and producing optimal solutions.

Although abundant researches have focused on the interval dominance relation, few studies have considered the crowding distance of interval numbers. Regarding the deterministic MOP, the traditional crowding distance (CD) was proposed in Nondominated Sorting Genetic Algorithm II (NSGAII) [45], which accounts to calculating the average distance of two individuals on either side along each of the objectives. For example, in Fig. 1(a), the CD of x_1 is infinite, shown as d_1, and the CD of x_2 is the average distance of x_1 and x_2 along f_1 and f_2, shown as d_2. In [46], the hypervolume-based crowding distance (HVCD) was presented and compared to the traditional CD, as shown in Fig. 1(b), demonstrating its capability of generating well-distributed set of solutions. More details can be found in this work [46]. Considering the IMOP, Hypervolume was chosen as the crowding distance in [38], where two distances, i.e., the worst and the best hypervolume, were used as selection criteria. However, situations in which the distances are not comparable may occur. In [38], the following strategy was employed to sort the whole population: (1) Compare individuals based on the rank assigned by the interval dominance relation; (2) Compare individuals based on the crowding distances assigned by hypervolume calculation; (3) Compare individuals randomly if the solutions cannot be distinguished by the above methods.

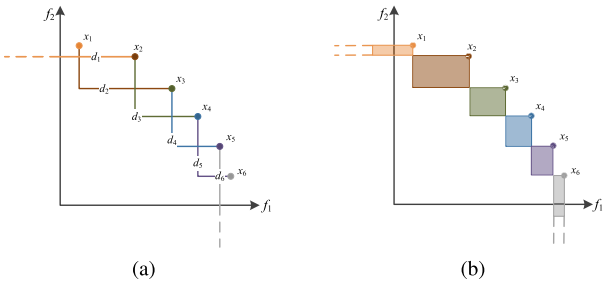

Fig. 1. Two cases of crowding distance: (a) The traditional crowding distance; (b) The Hypervolume-based crowding distance.

B. Review of Angle-Based Multi-Objective Optimization

The angle-based MOEAs can be classified into three categories, depending on the embedding position. The first category incorporates the angle into environmental selection. For instance, He *et al.* employed the Euclidean distance and angle as the measurement of convergence and diversity, respectively [47]. In their designed environmental selection, a pair of solutions with the minimum angle were found and, then, the representative solution with better convergence between them was identified. Besides, Yi *et al.* presented a vector angle-based MOEA, using the maximum-vector-angle-first for diversity and the worse-elimination principle for convergence [48]. The above methods treated the angle as the diversity measurement and followed the principle that the greater the angle, the better the population diversity. Different from that, Zhou *et al.* used the angle as a control parameter to keep a balance between convergence and diversity [49]. The second category embeds the angle into the dominance relation. For example, Ye *et al.* proposed a strengthened dominance relation considering the following two cases: (1) if the angle between a and b is lower than a pre-defined threshold and the convergence of a is better than b, a is dominant to b; (2) if the angle between a and b is more than a pre-defined threshold and the convergence of a is much better than b, a is dominant to b [50]. The third case considers both environmental selection and dominance relation. For example, Wang and Xu addressed the constrained problem with angle-based constrained dominance relation and angle-based diversity estimation [51]. In their method, it is obvious that the angle-based technique can not only intuitively reflect solution diversity, but also represent the (constraint) dominance relationship. The first category focuses more on the population distribution, the second on the interval dominance, and the third on a combination of the two, trying to achieve a balance between the population distribution and the interval dominance.

C. Motivation of This Study

The multi-objective RAPs have been proven to be NP-hard by Chern [52], which is difficult and time-consuming to be solved by traditional methods, especially when the system size is large [53]. Hence, a meta-heuristic algorithm should be specially tailored for obtaining the optimal solution. As discussed in Section II. A, there are few works considering the interval crowding distance. In [38], two HVCDs were calculated and a random sorting was performed when two individuals were not comparable. This method is relatively simple, but it cannot guarantee the effectiveness of the algorithm. Non-dominated sorting [45] of the two distances seems a good approach; however, it requires extra computational cost. Also, the transformation method is considered by calculating the distance of mid-points. However, as mentioned before, different transformation methods will bring out different results. Hence, an effective method with less extra computation cost is required for IMOPs, which motivates this paper. Since the angle-based technique reflects the distribution of solutions intuitively and there are no works considering the angle-based technique into IMOPs to our best knowledge, this paper tries to propose an effective interval crowding angle specially designed for the bi-objective redundancy allocation problem under interval uncertainty with no extra computation cost, which will be presented in Section IV. A. Furthermore, another motivation of this paper is to execute the optimization process and help DMs make a decision without considering preferences. Hence, a novel knee interval is proposed to select the most promising solution, which will be presented in Section IV. D.

III. System Description and Problem Formulation

For simplicity, a series-parallel system is considered consisting of n subsystems in series and x_i components arranged in parallel for the ith subsystem. Each component varies in different characteristics, i.e., reliability, cost, and weight, and adding redundant components can enhance the system reliability R_S but increase the system cost C_S at the same time. Therefore, the bi-objective RAP in an interval environment is formulated with the goal of minimizing the whole cost of the system while maintaining its reliability above a predetermined threshold.

A. Assumptions

Following [28], the assumptions for the interval RAP are as follows:

1) The characteristics of components, i.e., reliability, cost, or weight, are imprecise and interval-valued;
2) The failures of components are statistically independent of each other;
3) The multi-component system will not be damaged when a single component failure occurs;
4) When failures occur, the components and the whole system are assumed to be non-reparable;
5) All components and the system are supposed to be binary-state, i.e., only experiencing the perfectly functioning state and the completely failed state.

B. Formulation of Multi-Objective Interval RAP

Assuming that the type of components in a subsystem is identical, the interval-valued reliability of the ith subsystem of x_i components in parallel is defined as $[R_{iL}(x), R_{iR}(x)] = [1-(1-r_{iL})^{x_i}, 1-(1-r_{iR})^{x_i}]$, and the interval-reliability R_S of the system made of n such subsystems in series is [28], [31], [32], [54]–[56]:

$$R_S(x) = [R_{SL}(x), R_{SR}(x)] = \prod_{i=1}^{n} [R_{iL}(x), R_{iR}(x)] \tag{2}$$

To maximize the interval system reliability R_S and minimize the interval system cost C_S simultaneously, under the constraints g, the mathematical formulation is written as follows:

$$\begin{aligned} &max\, R_S \\ &min C_S \\ &s.t.\ g_k(x) \le 0, \quad k = 1, 2, \ldots, n_g \\ &\quad x_i \in Z^+, \quad i = 1, 2, \ldots, n \end{aligned} \tag{3}$$

where n_g represents the number of constrained functions.

IV. Proposed Approach

This paper proposes a novel method based on IP-MOEA and the interval crowding angle, here named as IP-ICA-MOEA. The pseudo-code of the proposed algorithm is given in Algorithm 1. It shares a common framework that is employed in many evolutionary algorithms, whether single objective or multiple objectives, deterministic values or interval values. The originalities introduced in this paper are indicated in italics in Algorithm 1. At first, a population P with size N, is initialized randomly in the decision space Ω. In what follows, the offspring population is generated by traditional genetic operators, i.e., crossover and mutation. In this paper, an elite selection for mutation is proposed to generate the offsprings with improved convergence and wider distribution. Since the size of population is fixed, N solutions are selected from S according to the rank obtained by IP-based non-dominated sorting [38] and crowding distance calculated by interval angle, where S is the union set of P and Q. The interval crowding angle is designed in this study specifically for the interval MOEA. The whole procedure repeats until the termination criterion is met, for example, the number of generations G reaches the maximum value G_{max}.

A. Interval Crowding Angle

As mentioned in Section II, the motivation of this study is to develop a novel crowding distance to reduce the calculation time and at the same time improve the calculation accuracy. For this purpose, an interval crowding angle is proposed in this paper for the interval MOEA, denoted as ICA, which can better estimate the diversity degree of the obtained solutions in the objective space. Before getting into ICA, the traditional calculation of the crowding angle for non-interval (i.e., deterministic) values is presented as follows. At first,

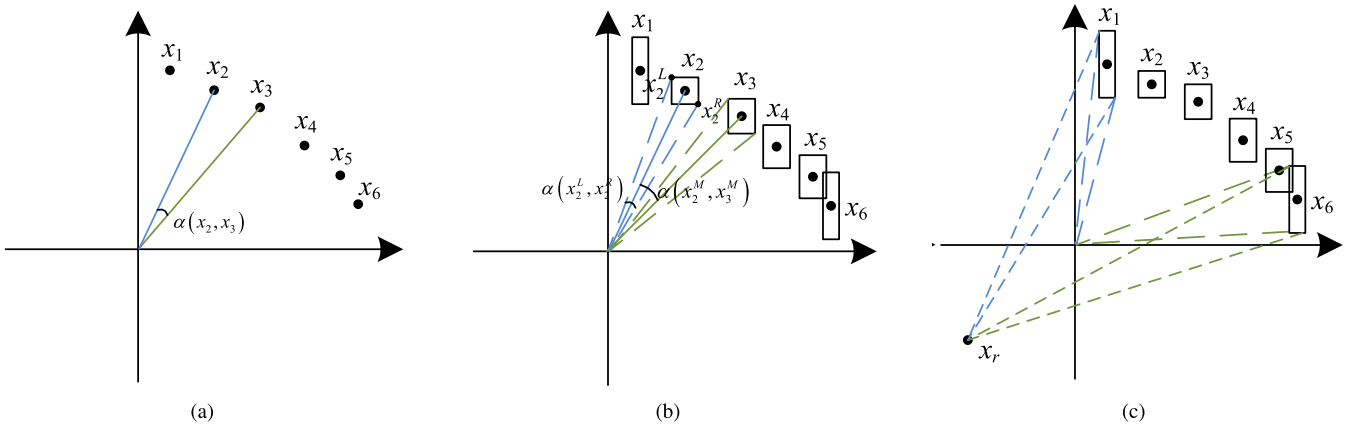

Fig. 2. Three cases of crowding angle: (a) The traditional crowding angle; (b) The interval crowding angle; (c) The interval crowding angle with new reference coordinate x_r.

Algorithm 1 IP-ICA-MOEA

```
Initialization population P;
G = 1;
while G ≤ G_max do
    Generate the offspring Q according to crossover, and elite mutation;
    S = P ∪ Q;
    Sort S according to IP-based non-dominated sorting and interval crowding angle;
    Select the new P from S, i.e., P = S[1, ..., N];
    G++;
end while
return P.
```

the normalization procedure is performed on the deterministic fitness values $f(x_i)$ of the ith solution x_i,

$$f'(x_i) = \frac{f(x_i) - min(f(x_i))}{max(f(x_i)) - min(f(x_i))} \tag{4}$$

As shown in many works [48], [51], the traditional crowding angle is defined as the angle between two adjacent vectors, denoted as $\alpha(x_i, x_j)$, using the following equation:

$$\alpha(x_i, x_j) = arccos|\frac{f'(x_i) \cdot f'(x_j)}{\|f'(x_i)\|_2 \times \|f'(x_j)\|_2}| \tag{5}$$

where $f'(x_i) \cdot f'(x_j)$ returns the inner product between the two normalized vectors, and $\|f'(x_i)\|_2$ is the norm of the vector of x_i, calculated as:

$$\|f'(x_i)\|_2 = \sqrt{\sum_{m=1}^{M} f'_m(x_i)^2} \tag{6}$$

Fig. 2(a) depicts the crowding angle between x_2 and x_3. However, this is not applicable for the interval MOEA because it considers only the angle between the midpoints, ignoring the interval distance. Therefore, to tackle this issue, this paper defines the crowding angle for interval MOEA with the following procedure. As before, the calculations are carried out in the normalized objective space and the normalization equation is given as:

$$f'(x_i, c) = \frac{f(x_i, c) - min(f(x_i, c))}{max(f(x_i, c)) - min(f(x_i, c))} \tag{7}$$

Since a bi-objective interval optimization problem is considered, we set the point $x_i^L = [min(f'_1(x_i, c)), max(f'_2(x_i, c)]$ as the left point of x_i, and $x_i^R = [max(f'_1(x_i, c)), min(f'_2(x_i, c)]$ as its right point. Thus, the interval angle of $f'(x_i, c)$ is given as $\alpha(x_i^L, x_i^R)$, which can be computed via (5). Taking x_2 in Fig. 2(b) as an example, x_2^L is its left point, x_2^R is its right point, and $\alpha(x_2^L, x_2^R)$ is its interval angle. It is obvious from the figure that the interval angle depicts the interval range of the individual. On this basis, the interval crowding angle can be defined as follows.

$$\alpha_I(x_i, x_j) = \frac{\alpha(x_i^M, x_j^M)}{\alpha(x_i^L, x_i^R) + \alpha(x_j^L, x_j^R)} \tag{8}$$

where x_i^M denotes the mid-point of x, given by:

$$x_i^M = [\frac{min(f'_1(x_i, c)) + max(f'_1(x_i, c))}{2}, \frac{min(f'_2(x_i, c)) + max(f'_2(x_i, c))}{2}] \tag{9}$$

Using α_I, not only the angle between the mid-points is considered, but also the interval angle ranges of both individuals are taken into account. However, carrying out some pre-experiments, the results are not satisfactory. As shown in Fig. 2(c), it seems that x_1 and x_6 should have the same range of interval angle. If taking (0,0) as the reference coordinate, $\alpha_I(x_1^L, x_1^R)$ is significantly less than $\alpha_I(x_6^L, x_6^R)$ using (8), which is not consistent with the actual situation. To solve this issue, this paper selects a new reference coordinate, denoted as x_r. Thus, the interval angle of x_i is computed as $\alpha(x_i^L - x_r, x_i^R - x_r)$, the angle between x_i and x_j is given as $\alpha(x_i^M - x_r, x_j^M - x_r)$, and the final calculation of ICA is further modified as (10), with respect to the reference point x_r. Comparing (8) and (10), the former is a specific form of the latter when $x_r = [0, 0]$. Hence, the selection of x_r is

rather important for the performance of ICA, which is further discussed in the experiment section.

$$\alpha_I(x_i, x_j) = \frac{\alpha(x_i^M - x_r, x_j^M - x_r)}{\alpha(x_i^L - x_r, x_i^R - x_r) + \alpha(x_j^L - x_r, x_j^R - x_r)} \tag{10}$$

As mentioned in Section II, the angle-based technique reflects distribution of solutions. To be specific, the major benefits of the proposed ICA are described as follows:

1) The proposed ICA is especially designed for the interval MOEAs, considering not only the angle between two compared individuals but also the angle range of the interval values;
2) Since it is difficult to sort the population based on two distances obtained by the existing methods [46], non-dominated sorting is performed to sort the population, with extra computational cost. Only one crowding distance is achieved by this approach, greatly reducing the computation time. This advantage is verified by the analysis of the T metric in the experiment section;
3) The proposed ICA is very competitive compared with other existing methods to estimate the distribution of solutions, which is also demonstrated in the experiment section.

B. Elite Selection for Mutation

Considering the mutation operator, the whole population is selected in the original IP-MOEA. However, it is not necessary to keep the individuals with bad convergence and distribution in the population. Hence, this paper chooses the elite solutions (the top $e \times N$ individuals) for mutation, given by the population sorted according to the rank obtained by IP-based non-dominated sorting and interval crowding angle, where e represents the rate of elite selection. The most significant benefit of this is that the potential solution with good convergence and wide distribution has more chance to retain the population and generate improved offsprings. The value of e is further discussed in the experimental section for showing its effectiveness.

C. Constraint Handling

For guiding the search toward feasible regions and taking the constraints into consideration, it is common to use a penalty function, referring to [2], [57], [58]. On the basis of (1), the problem is converted to an unconstrained problem with the penalty-guided constraint handling technique:

$$max f(x, c) + v_g g(x) + v_h h(x) \tag{11}$$

where v_g and v_h are penalty coefficients.

D. Knee Interval Analysis

Applying the proposed algorithm, a set of Pareto solutions is obtained for DMs to choose. However, if no preference is provided, knee point analysis is presented to help DMs to select the most promising solution among the Pareto optimal front for precise solutions. The knee point refers to the point with the maximum marginal rates of return, meaning that there is a small improvement in one objective, accompanied by severe degradation of at least one other objective [59]. As proved by [60], the knee point has the best hypervolume metric among all Pareto solutions. Different from the current researches concentrating on the precise problems, this paper tries to find the knee point among interval solutions, named knee interval. First, knee points are calculated for lower points and upper points, respectively. Since there are many definitions of this point, this paper refers to the definition of [59]–[61]. The mathematical formula of straight line l is as follows:

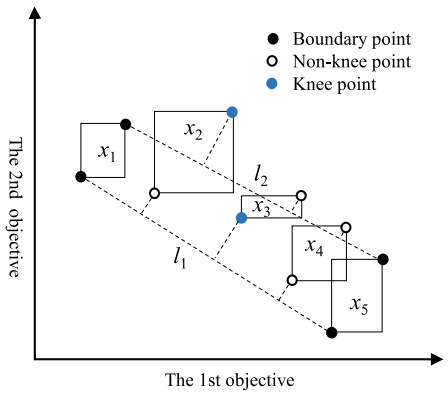

Fig. 3. The knee interval analysis of the multi-objective interval optimization problem.

$$ax + by + c = 0 \tag{12}$$

The point k with the coordinate (x_k, y_k), so the distance of the point k to the line l is as follows:

$$d(k, l) = \frac{|ax_k + by_k + c|}{\sqrt{a^2 + b^2}} \tag{13}$$

Then, imprecision is used as a second comparison criterion when the distances stay incomparable. For the interval optimization problem, the solution with the least imprecision is the most promising one. Take Fig. 3 as an example, x_3 has the largest distance to l_1 and x_2 has the largest distance to l_2. As a consequence, x_3 is selected as the optimal solution for DMs with less imprecision. In the proposed method, the solution with larger hypervolume value and less imprecision is the knee interval, more details about hypervolume and imprecision can refer to Section V. B.

E. Computational Complexity Analysis

The complexity of the proposed algorithm IP-ICA-MOEA is compared with that of the original algorithm IP-MOEA for each generation. Since both of them adopt the same non-dominance-sorting method, the computation complexity is $O(MN^2)$ in the worst cases [62], where M is the number of objectives, and N is the population size. Although IP-ICA-MOEA and IP-MOEA utilize different estimation methods of interval crowding distance (angle-based and hypervolume-based, respectively), the main part is sorting in the ascending order according to the objective values and the complexity is $O(MNlogN)$. The significant difference between them is

TABLE I
DATA FOR EXAMPLE 1

i	1	2	3	4	5
r_i	[0.78, 0.82]	[0.84,0.85]	[0.87,0.91]	[0.63,0.66]	[0.74,0.76]
c_i	[6, 8]	[5,8]	[3,6]	[6,9]	[3,6]
p_i	1	2	3	4	2
w_i	7	8	8	6	9

$b_1 = 110, b_2 = 200$

TABLE II
DATA FOR AVAILABLE COMPONENT TYPES FOR EXAMPLE 2

Type j	Subsystem $i=1$		Subsystem $i=2$		Subsystem $i=3$	
	r_{ij}	c_{ij}	r_{ij}	c_{ij}	r_{ij}	c_{ij}
1	[0.93, 0.95]	[8, 10]	[0.96, 0.98]	[11, 13]	[0.95, 0.97]	[9, 11]
2	[0.90, 0.92]	[5, 7]	[0.85, 0.87]	[2, 4]	[0.88, 0.90]	[5, 7]
3	[0.88, 0.90]	[5, 7]	[0.69, 0.71]	[1, 3]	[0.71, 0.73]	[3, 5]
4	[0.74, 0.76]	[2, 4]	[0.65, 0.67]	[1, 3]	[0.70, 0.72]	[2, 4]
5	[0.71, 0.73]	[1, 3]			[0.66, 0.68]	[1, 3]

the selection guided by the crowding distance. Because there are two distances obtained by IP-MOEA, random sorting cannot guarantee the effectiveness. The non-dominance-sorting method is used to compare the distances and the complexity is $O(N^2)$. Instead, only one distance is obtained by ICA in IP-ICA-MOEA. Hence, the complexity reduces to $O(NlogN)$ in the worst cases.

V. EXPERIMENTAL RESULTS

This section is devoted to the experimental study for analyzing the performance of the proposed IP-ICA-MOEA including four groups of analysis. The first group aims to tune the parameters, analyzing the influence of different parameter values. The aim of the second group is to investigate the effects of the originalities proposed in this paper. In the third group, a comprehensive comparison between IP-ICA-MOEA and other four state-of-the-art methods is conducted. The analysis of knee interval is presented in the last group. All algorithms are run on: Intel (R) Core(TM) i5-6500 CPU, 3.20 GHz, 8 GB RAM, Windows 7, and MATLAB R2014a.

A. Reliability Optimization Problems

Two classical test problems taken from [28] are chosen for our empirical studies with interval-valued data of components (Table I and II).

Example 1: The first example considers a typical series-parallel system taken from [31], consisting of five subsystems in series. For each subsystem, the type of the components in parallel is identical. The structure diagram of the referred system is provided as Fig. 4(a).

$$max\, R_S = [R_{SL}, R_{SR}] = \prod_{i=1}^{5} [1 - [1 - r_{iR}, 1 - r_{iL}]^{x_i}]$$

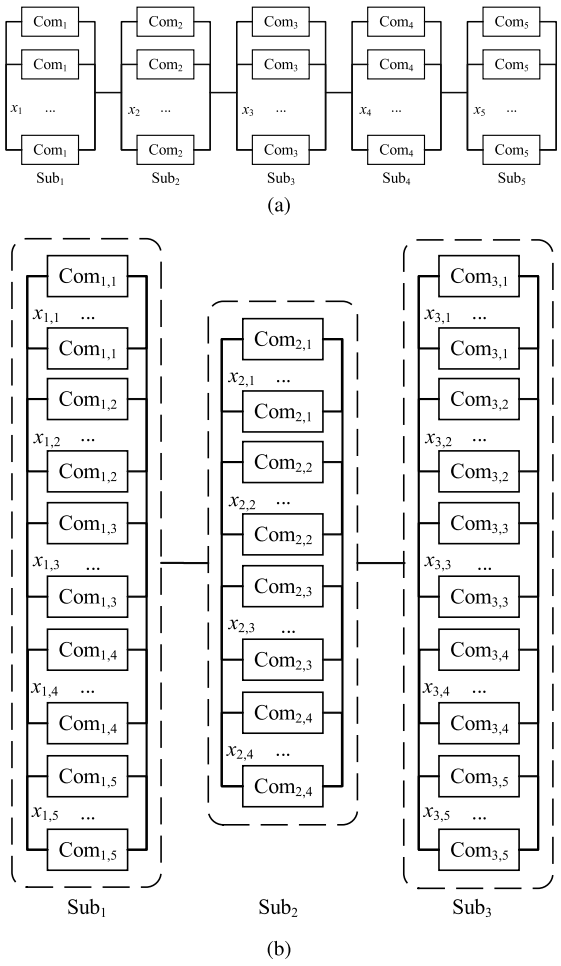

Fig. 4. The structure diagram of the referred systems. (a) Example 1; (b) Example 2.

$$\begin{aligned} min C_S &= [C_{SL}, C_{SR}] = \sum_{i=1}^{5} [c_{iL}, c_{iR}][x_i + exp(\frac{x_i}{4})] \\ s.t.\ g_1(x) &= \sum_{i=1}^{5} p_i x_i^2 - b_1 \le 0 \\ g_2(x) &= \sum_{i=1}^{5} w_i [x_i + exp(\frac{x_i}{4})] - b_2 \le 0 \end{aligned} \tag{14}$$

where x_i is the decision variable representing the number of components in subsystem i, $[R_{SL}, R_{SR}]$ and $[C_{SL}, C_{SR}]$ are the interval form of the system reliability and cost respectively, $[r_{iL}, r_{iR}]$ and $[c_{iL}, c_{iR}]$ are the interval reliability and cost of component i respectively. The data for Example 1, including the values of r_i, c_i, p_i, w_i, b_1 and b_2, is listed in Table I. Besides, g_1 is the limitation on the sum of the subsystems' products by weight and square of the volume and g_2 denotes the constraint for the weight of the system. By applying the penalty-guided constraint handling technique, the mathematical model is converted into the unconstrained one, by maximizing $R_s - max(0, g_1) - max(0, g_2)$ and $-C_s - max(0, g_1) - max(0, g_2)$.

Example 2: A system with three subsystems in series and an option of different component types in each subsystem is

considered in the second example, as shown in Fig. 4(b).

$$\begin{aligned} &max\, R_S = [R_{SL}, R_{SR}] = \prod_{i=1}^{3}[1 - \prod_{j=1}^{m_i}[1 - r_{ijR}, 1 - r_{ijL}]^{x_i}] \\ &min C_S = [C_{SL}, C_{SR}] = \sum_{i=1}^{3}\prod_{j=1}^{m_i}[C_{ijL}, C_{ijR}]x_{ij} \\ &s.t.\ 1 \le \prod_{j=1}^{m_i} x_{ij} \le n_{max,i} \end{aligned} \tag{15}$$

where x_{ij} is the decision variable denoting the number of jth-type component used in subsystem i, $[r_{ijL}, r_{ijR}]$ and $[c_{ijL}, c_{ijR}]$ are the interval reliability and cost of jth component in ith subsystem respectively, m_i is the number of available component types in the ith subsystem, and $n_{max,i}$ denotes the maximum number of components selected in subsystem i, set to 8 as suggested in [28]. More details of the available component types are presented in Table II.

B. Performance Indicators

The following four indicators are employed for comparisons from different views.

1) The number of feasible solutions in the Pareto set (NF metric, for short). This indicator is suggested in this paper to compare the number of non-repeating solutions in the Pareto set. As known, there may be duplicate solutions in the Pareto set. Hence, the larger the value of the NF metric, the better the algorithm;
2) Midpoint hypervolume (mH metric, for short). Hypervolume is a comprehensive metric considering both convergence and spread for MOEA [63]. For the interval MOEA, midpoint hypervolume was introduced to reflect the approximation performance of the nondominated set in [38]. A greater value of mH indicates both a better convergence and a good distribution of the solutions. The hypervolume needs a reference point for closing the volume, e.g. multiplying the worst objective values by 20% [64]. In our case, this reference point is set to [-0.2, -0.2];
3) Imprecision (I metric, for short). In order to evaluate the average uncertainty, the I metric is calculated by the product of the interval widths for all nondominated solutions, as shown in [38];
4) CPU time (T metric, for short). The smaller the T value, the higher the computational efficiency of the algorithm.

C. Parameter Calibration

Before getting started to parameter calibration, the size of population n_{pop} and the number of maximum allowable iterations per run G_{max} are declared as suggested in [28]: $n_{pop} = 30$ and $G_{max} = 50$ for Example 1, and $n_{pop} = 50$ and $G_{max} = 100$ for Example 2. Following that, two genetic operators (crossover and mutation) are employed to generate offsprings for the considered problem. Since the number of the components is the decision variable, the genetic operators should be discretized as follows:

$$\begin{aligned} [y_{1,1}, y_{1,2}, \ldots, y_{1,v}] &= \beta \cdot [x_{1,1}, x_{1,2}, \ldots, x_{1,v}] \\ &\quad + (1 - \beta) \cdot [x_{2,1}, x_{2,2}, \ldots, x_{2,v}] \\ [y_{2,1}, y_{2,2}, \ldots, y_{2,v}] &= (1 - \beta) \cdot [x_{1,1}, x_{1,2}, \ldots, x_{1,v}] \\ &\quad + \beta \cdot [x_{2,1}, x_{2,2}, \ldots, x_{2,v}] \end{aligned} \tag{16}$$

where $[x_{1,1}, x_{1,2}, \ldots, x_{1,v}]$ and $[x_{2,1}, x_{2,2}, \ldots, x_{2,v}]$ are two parents, v is the dimension of the solutions, and $[y_{1,1}, y_{1,2}, \ldots, y_{1,v}]$ and $[y_{2,1}, y_{2,2}, \ldots, y_{2,v}]$ are two offsprings generated by the crossover operator. Besides, β is a binary vector which is generated randomly. Because the occurrence probability of crossover is typically much larger than that of mutation [65], the probability of crossover is set to 0.9 and the probability of mutation is set to 0.1. Considering the discrete mutation, the value of the mutation index is first set as $\lceil 0.02 \times v \rceil$, and the mutation step is $\lfloor 0.7 \times randn \rfloor$, where $randn$ conforms to a normal distribution with mean 0 and variance 1, $\lceil \cdot \rceil$ and $\lfloor \cdot \rfloor$ represent the ceil and floor functions, respectively.

For demonstrating the influence of parameters, parameter tuning is performed in this section with 30 independent runs. As stated in Section IV, the proposed IP-ICA-MOEA contains the interval crowding angle and elite selection for mutation compared to the original IP-MOEA. Therefore, the following key control factors are considered, i.e., angle reference coordinate x_r and elite rate for mutation e. The values of each parameter are set according to some preliminary experiments. For x_r, all objective values are normalized to [0, 1]. Hence the lowest objective coordinated is [0, 0]. Similar to the approach of deciding the reference point of mH, the rest available reference coordinate is set to [-0.5, -0.5] and [-1, -1]. Meanwhile, the elite rate for mutation e is tested on five levels $\{0.2, 0.4, 0.6, 0.8, 1.0\}$, where 1.0 means selecting the whole population for mutation whereas 0.2 denotes that only the top part of individuals are selected for mutation. The boxplots of the four metrics (NF, mH, I, and T) obtained with different parameter values are shown as in Fig. 5 and 6, where the central mark of the box indicates the median, and the bottom and top edges indicate the 25th and 75th percentiles, respectively.

1) Parameter calibration of x_r: Fig. 5 depicts the boxplots of the four metrics obtained with different x_r values in the two examples. Considering the NF metric, the number of non-repeating individuals is very close. For mH, it is obvious that $[-0.5, -0.5]$ yields a larger median and bottom edge than the other methods, and the top edges of the three values are the same, which indicates the performance of $[-0.5, -0.5]$ in terms of convergence and diversity. Fig. 5(c) shows the median value obtained by $[-0.5, -0.5]$ is the lowest on Example 1 among all values, and lower than $[-0, -0]$ on Example 2. Similarly, $[-0.5, -0.5]$ yields the lower median value than $[-0, -0]$ on Example 1 and the lowest median value on Example 2 among all values, as shown in Fig. 5(d). These results show that $[-0.5, -0.5]$ is better than $[-0, -0]$ and competitive to $[-1, -1]$ in terms of I and T, respectively. To sum up, the reference point [0, 0] obtains the worst results, whereas $[-0.5, -0.5]$ achieves better results (mH, I on Example 1 and NF, mH, T on Example 2) in 5 out of 8 cases. These results are consistent with the analysis from Fig. 2. Regarding to the computation of α_I, (8) is a special case of (10) when $x_r = [-0, -0]$. However,

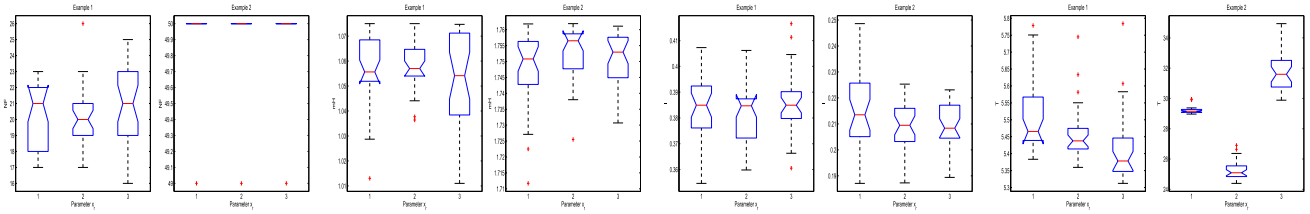

(a) (b) (c) (d)

Fig. 5. Boxplots of parameter x_r over 30 times: (a) Boxplots of NF on Example 1 and Example 2; (b) Boxplots of mH on Example 1 and Example 2; (c) Boxplots of I on Example 1 and Example 2; (d) Boxplots of T on Example 1 and Example 2. (1: $x_r = [0, 0]$, 2: $x_r = [-0.5, -0.5]$, 3: $x_r = [-1.0, -1.0]$.)

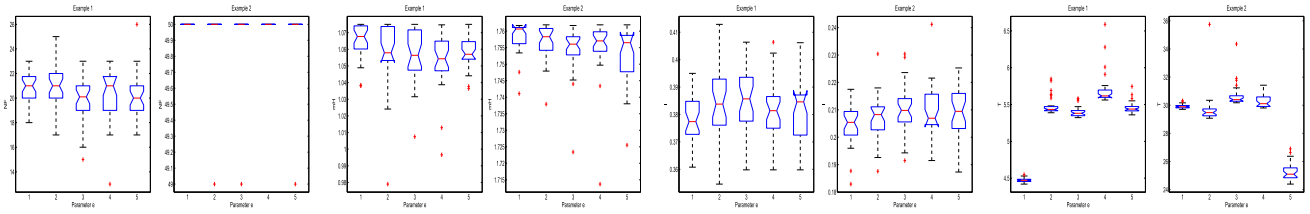

(a) (b) (c) (d)

Fig. 6. Boxplots of parameter e over 30 times: (a) Boxplots of NF on Example 1 and Example 2; (b) Boxplots of mH on Example 1 and Example 2; (c) Boxplots of I on Example 1 and Example 2; (d) Boxplots of T on Example 1 and Example 2. (1: $e = 0.2$, 2: $e = 0.4$, 3: $e = 0.6$, 4: $e = 0.8$, 5: $e = 1.0$.)

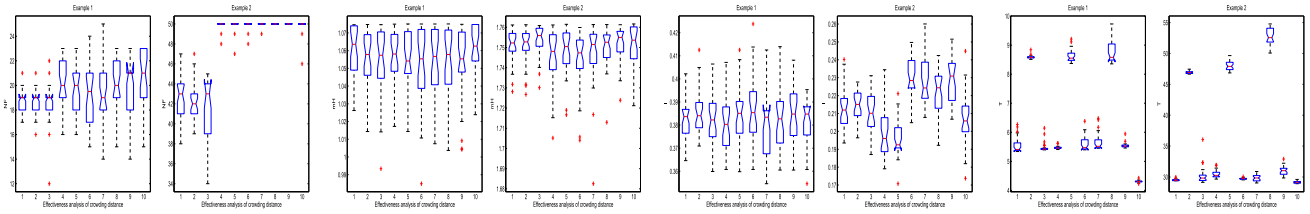

(a) (b) (c) (d)

Fig. 7. Boxplots of effectiveness analysis of CD over 30 times: (a) Boxplots of NF on Example 1 and Example 2; (b) Boxplots of mH on Example 1 and Example 2; (c) Boxplots of I on Example 1 and Example 2; (d) Boxplots of T on Example 1 and Example 2. (Combination 1: CD with MID, Combination 2: CD with NDS, Combination 3: CD with RS, Combination 4: HVCD with MID, Combination 5: HVCD with NDS, Combination 6:HVCD with RS, Combination 7: CA with MID, Combination 8: CA with NDS, Combination 9: CA with RS, and Combination 10: ICA).

if $[-0, -0]$ is chosen as the reference point, the interval angle range is not correct. Hence, the reference point is set to $[-0.5, -0.5]$.

2) Parameter calibration of e: Fig. 6 depicts the boxplots of the four metrics obtained by different values of e in the two examples. From Fig. 6 (b, the median value of the mH achieved by 0.2 is the largest and the median value of I obtained by 0.2 is the lowest on both examples, which demonstrates the effectiveness of $e = 0.2$ in terms of convergence, diversity, and imprecision. Regarding the rest of the metrics, the results obtained by 0.2 have a competitive performance as well. As a consequence, 6 out of 8 median values (except NF on Example 1 and T on Example 2) are the best among all considered values. Therefore, the factor e is set to 0.2 due to its effectiveness.

D. Effectiveness Analysis

The proposed IP-ICA-MOEA contains two main operators: (1) interval crowding angle; (2) elite mutation. To verify the performance of the proposed ICA, it is compared with the original crowding distance (CD), the Hypervolume-based crowding distance (HVCD), and the crowding angle (CA), as detailed in Section II. For IMOPs, there may be a case in which it is impossible to compare two distances. Hence, the following strategies, i.e, converting the two distances into one distance by calculating the distance between mid-points (MID), non-dominated sorting (NDS), and randomly sorting (RS), are combined in the algorithm to demonstrate the effects on the final results. To be specific, the first strategy differs from the latter two in that the former calculates only one distance, whereas the latter two calculate two distances and differentiate between individuals by means of sorting. To make a fair comparison, each combination is performed 30 times independently. All parameters for each improvement are set to the same expression as Section V. C. The results depicted as boxplots obtained by different CDs are given in Fig. 7, and the effectiveness analysis of CD is as follows:

1) From the perspective of NF metric, Combinations 1-3 yield the worst median results on both cases, which indicates that no matter the way of employing MID, NDS,

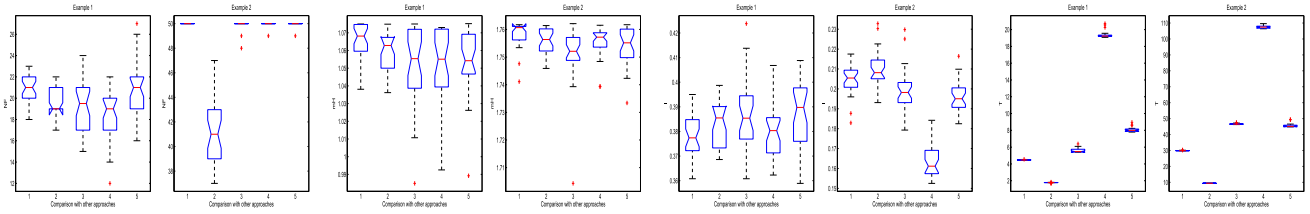

(a) (b) (c) (d)

Fig. 8. Boxplots of comparison with other approaches over 30 times: (a) Boxplots of NF on Example 1 and Example 2; (b) Boxplots of mH on Example 1 and Example 2; (c) Boxplots of I on Example 1 and Example 2; (d) Boxplots of T on Example 1 and Example 2. (Algorithm 1: IP-ICA-MOEA, Algorithm 2: IP-MOEA, Algorithm 3: IC-MOEA, Algorithm 4: MI-NOEA, Algorithm 5: Mid-NSGAII).

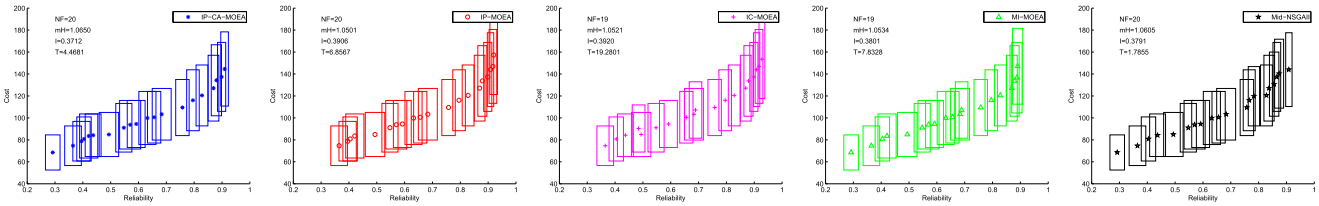

(a) (b) (c) (d) (e)

Fig. 9. The distribution of solutions obtained by all compared algorithms on Example 1: (a) IP-ICA-MOEA; (b) IP-MOEA; (c) IC-MOEA; (d) MI-MOEA; (e) Mid-NSGAII.

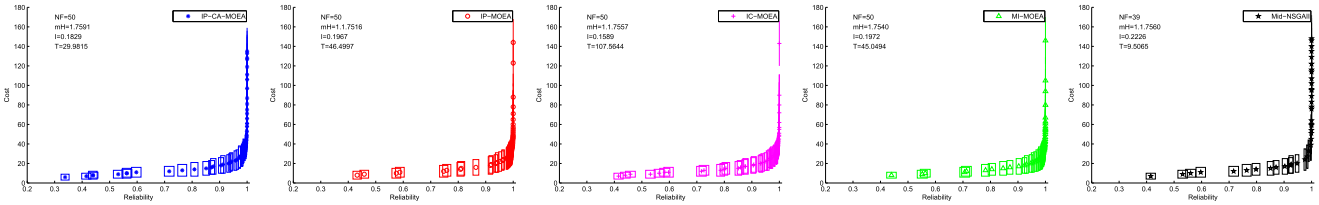

(a) (b) (c) (d) (e)

Fig. 10. The distribution of solutions obtained by all compared algorithms on Example 2: (a) IP-ICA-MOEA; (b) IP-MOEA; (c) IC-MOEA; (d) MI-MOEA; (e) Mid-NSGAII.

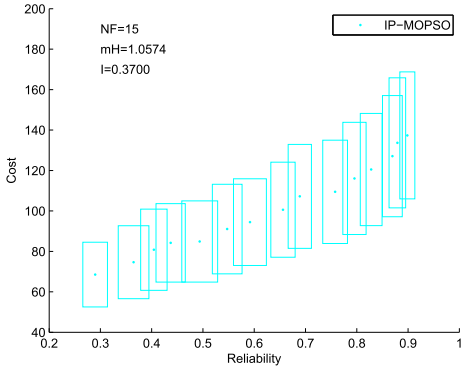

Fig. 11. The distribution of solutions recorded by IP-MOPSO on Example 1.

and RS, the traditional CD generates more repeating individuals than other CDs. On Example 1, the median of NF obtained by Combination 10 is higher than that from other combinations, and on Example 2, it is equal to that obtained by Combinations 4-9. Hence, it can be concluded that solutions obtained by ICA are rarely duplicated;

2) mH and I are important metrics to evaluate convergence, diversity, and imprecision. As shown from Fig. 7 (b), ICA yields the best median results on all cases, except Combination 1 on Example 1 and Combinations 3 and 9 on Example 2. Combination 3 is CD with RS, Combination 9 is CA with RS, both of them sort the non-comparable individuals randomly. It is also obvious that ICA has a good performance on Example 2 (7 out of 9 results) from Fig. 7(c). Above all, ICA is competitive among all combinations;
3) In terms of computational efficiency, the intervals obtained by ICA are below the others, which verifies that ICA is significantly better than other combinations on both examples. Among all combinations, Combinations 2, 5, and 8 need more computational time to perform non-dominated sorting. The mean values of T obtained by the different combinations are listed in Table III, where the improvement is calculated by $\frac{T_i - T_{10}}{T_i}$, $i \in [1, 9]$. As been from the table, ICA reduces the average computing time by at least 21.27% and 1.89%

TABLE III
MEAN VALUES OF T OBTAINED BY DIFFERENT COMBINATIONS

Combination	Example 1		Example 2	
	$T(s)$	Improvement	$T(s)$	Improvement
1	5.55	22.34%	29.50	1.18%
2	8.59	49.81%	46.94	37.89%
3	5.48	21.40%	30.23	3.55%
4	5.47	21.27%	30.44	4.22%
5	8.62	50.03%	48.00	39.26%
6	5.59	22.97%	29.72	1.90%
7	5.66	23.88%	29.86	2.35%
8	8.77	50.87%	52.76	44.74%
9	5.54	22.27%	31.01	5.97%
10	4.31		29.15	

on the two examples, compared to the other methods, respectively.

Hence, the proposed ICA is capable of obtaining a Pareto optimal set with good performance, generating less non-repeating individuals, faster convergence, better diversity, less imprecision, and reduced running time. Furthermore, the effectiveness analysis of elite mutation can be seen from Fig. 6, where the factor e represents the elite rate for mutation. The case ($e = 1.0$) indicates that elite mutation is not performed and the case ($e = 0.2$) obtains the best results as found from the analysis of parameter calibration. Thus, the improvement of elite mutation is also effective for the proposed algorithm.

E. Comparison With Other Approaches

For the purpose of performance comparison, the proposed algorithm has been compared with several state-of-the-art variants of IP-MOEA as well. These well-known algorithms are as follows: the basic IP-MOEA [38], credibility-based IC-MOEA [40], MI-MOEA [43] with possibility degree, Mid-NSGAII with midpoints by transforming the interval number to a deterministic one [35]. The compared algorithms are strictly re-implemented with the same programming in the same environment and parameters. For a fair comparison, each algorithm is run 30 times for each instance. The comparisons of these well-known approaches are given in Fig. 8.

It is obvious from Fig. 8(a) that the medium values of the NF metric obtained by the proposed IP-ICA-MOEA are good on both Examples. Especially for Example 2, there are no repeating individuals in the Pareto Front achieved by IP-ICA-MOEA, which verifies the effectiveness of finding non-repeating individuals. Considering mH metric, IP-ICA-MOEA yields the best median results on both Examples. Besides, the notches of IP-ICA-MOEA are not overlapped with all considered algorithms on Example 2, which verifies that IP-ICA-MOEA is significantly better than other approaches on Example 2 in terms of convergence and distribution. It is obvious from Fig. 8(c) that IP-ICA-MOEA obtains the best median results on Example 1, which illustrates its competitiveness on generating solutions with less imprecision.

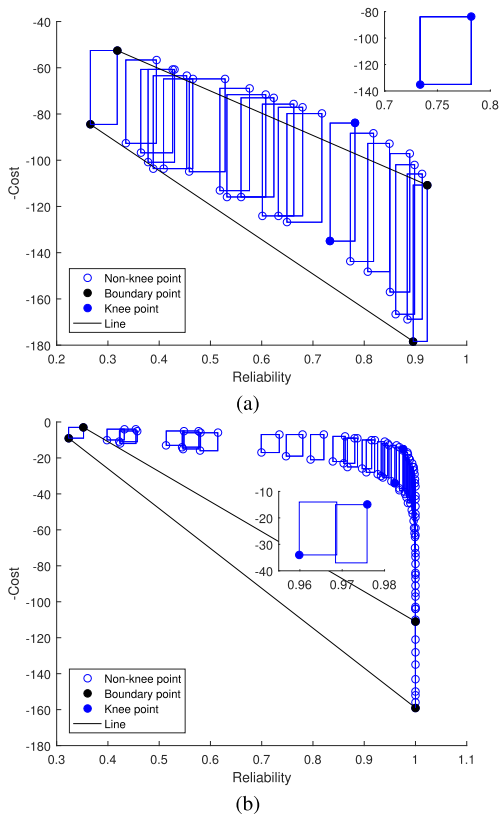

Fig. 12. The knee interval analysis of the referred systems. (a) Example 1; (b) Example 2.

From the perspective of running time T, Mid-NSGAII replaces the interval numbers by the mid-points without the dominant calculation of interval values: hence, it takes the least time among all algorithms. Compared with other MOEAs considering the interval dominance relation, the proposed IP-ICA-MOEA spends the least computational time. To sum up, the experiment results demonstrate that the proposed algorithm is powerful and more efficient than other state-of-the-arts on this sort of problems.

Furthermore, to visually understand the distribution of the obtained solutions, this paper plots the comparisons of results obtained by all algorithms in Fig. 9 and Fig. 10. Besides, the recorded results obtained by IP-MOPSO are also shown in Fig. 11 for Example 1. Since 30 independent runs are performed, we choose the population where mH is closest to its mean for a fair comparison. As clearly seen from Fig. 9 and Fig. 11, the lower reliabilties of IP-MOEA and IC-MOEA are larger than 0.3, and the upper costs are more than 180, indicating the tendency to find the solutions with high reliability and cost. Among all algorithms, NF obtained by IP-MOPSO is the lowest, which shows the effectiveness of the framework of GA. The significant superiority of IP-ICA-MOEA can be seen from Fig. 10: only the interval reliability of IP-ICA-MOEA is lower than 0.4, and its solution is more widely and uniformly distributed than that obtained by other algorithms when the reliability is close to 1, except Mid-NSGAII. However, the number of non-repeating Pareto solutions obtained by Mid-NSGAII is the least. Hence, we can conclude that the proposed

algorithm produces well-distributed Pareto fronts due to the superiority of the angled-based mechanism.

F. Knee Interval Analysis

Without the extra knowledge of preferences on uncertainties, a novel knee interval analysis is proposed in this paper to help DMs to select the best solution among a set of Pareto Front, as given in Fig 12. As from Fig 12(a), the solution $[2, 2, 2, 2, 2]$ with interval reliability $[0.7336, 0.7819]$ and cost $[83.9206, 135.0027]$ is the knee interval, which has the largest HV among all solutions for Example 1. As from Fig 12(b), there are two knee intervals: the solution $[0, 0, 0, 1, 2, 0, 2, 1, 0, 0, 0, 0, 1, 3]$ with interval reliability $[0.9599, 0.9687]$ and cost $[14, 34]$,and the solution $[0, 0, 0, 2, 2, 0, 1, 2, 0, 0, 0, 0, 1, 3]$ with interval reliability $[0.9684, 0.9759]$ and cost $[15, 37]$. The Im of the first solution is 0.1413 and that of the second one is 0.1520. Hence, the first solution is the knee interval for Example 2, which has the larger HV and less Im.

VI. Conclusion

An interval bi-objective redundancy allocation problem is formulated, aiming at minimizing the system cost and maximizing the system reliability, under several pre-defined constraints. To our best knowledge, it is the first time that an angle-based technique is proposed for tackling the issue of estimating the interval crowding distance. As verified in experiments, the proposed approach describes the distribution of population effectively. Besides, guided by this mechanism, the complexity of selection is reduced to $O(NlogN)$ from $O(N^2)$ in the worst cases. As a consequence, ICA can decrease the average running time by at least 21.27% and 1.89% on both cases compared to the other methods, respectively. Then, this paper employs the elite selection for mutation and penalty guided constraint handling for obtaining an improved population and dealing with the constraints, respectively. Experiment results demonstrate that the proposed IP-ICA-MOEA achieves significantly better performance compared with other state-of-the-art algorithms. Furthermore, this paper selects the optimal solution among a set of Pareto solutions to help DMs make a decision, using the proposed knee interval calculation.

Future work, with both practical and theoretical perspectives, can be summarized as the following four directions:

1) This study focuses on minimizing system cost and maximizing system reliability, and the number of objective functions is set to 2. The feasibility and effectiveness of ICA is not verified when the number of objective functions increases ($M \geq 3$). Hence, we will extend this direction in the future for the calculation of angles between two individuals in high dimensional cases;
2) The experimental examples are all in the series-parallel configurations. Since the approach is applicable for any type of systems, extensive experiments from different types of systems will be carried out via the proposed algorithm. Along this direction, practical systems will be considered, such as multi-state, multi-level, redundancy strategy, and etc;
3) As known from the concept of interval optimization, the constraints are imprecise in some situations. The interval constraints should be considered in future work. It is worth noting that [51] has proposed the angle-based algorithm with infeasibility information, maybe it is feasible to design an interval angle for constrainted problems;
4) We believe IC-ICA-MOEA can be applied (embedded) into all MOEAs to estimate the interval crowding distance. Furthermore, we notice that lots of benchmarks have been presented in [38]: more experiments should be performed to verify performance.

References

[1] L. Zia and D. W. Coit, "Redundancy allocation for series-parallel systems using a column generation approach," *IEEE Trans. Rel.*, vol. 59, no. 4, pp. 706–717, Dec. 2010.
[2] Y. Xu and D. Pi, "A hybrid enhanced bat algorithm for the generalized redundancy allocation problem," *Swarm Evol. Comput.*, vol. 50, Nov. 2019, Art. no. 100562.
[3] X.-Y. Li, Y.-F. Li, and H.-Z. Huang, "Redundancy allocation problem of phased-mission system with non-exponential components and mixed redundancy strategy," *Rel. Eng. Syst. Saf.*, vol. 199, Jul. 2020, Art. no. 106903.
[4] Y. Xu, D. Pi, S. Yang, and Y. Chen, "A novel discrete bat algorithm for heterogeneous redundancy allocation of multi-state systems subject to probabilistic common-cause failure," *Rel. Eng. Syst. Saf.*, vol. 208, Apr. 2021, Art. no. 107338.
[5] A. E. Baladeh and E. Zio, "A two-stage stochastic programming model of component test plan and redundancy allocation for system reliability optimization," *IEEE Trans. Rel.*, vol. 70, no. 1, pp. 99–109, Mar. 2020.
[6] W. Shao, D. Pi, and Z. Shao, "A Pareto-based estimation of distribution algorithm for solving multiobjective distributed no-wait flow-shop scheduling problem with sequence-dependent setup time," *IEEE Trans. Autom. Sci. Eng. (from July 2004)*, vol. 16, no. 3, pp. 1344–1360, Jul. 2019.
[7] D. Cao, A. Murat, and R. B. Chinnam, "Efficient exact optimization of multi-objective redundancy allocation problems in series-parallel systems," *Rel. Eng. Syst. Saf.*, vol. 111, pp. 154–163, Mar. 2013.
[8] R. Kumar, K. Izui, M. Yoshimura, and S. Nishiwaki, "Multi-objective hierarchical genetic algorithms for multilevel redundancy allocation optimization," *Rel. Eng. Syst. Saf.*, vol. 94, no. 4, pp. 891–904, Apr. 2009.
[9] A. Chambari, P. Azimi, and A. A. Najafi, "A bi-objective simulation-based optimization algorithm for redundancy allocation problem in series-parallel systems," *Expert Syst. Appl.*, vol. 173, Jul. 2021, Art. no. 114745.
[10] E. Zio and R. Bazzo, "Level diagrams analysis of Pareto front for multiobjective system redundancy allocation," *Rel. Eng. Syst. Saf.*, vol. 96, no. 5, pp. 569–580, May 2011.
[11] K. Govindan, A. Jafarian, M. E. Azbari, and T.-M. Choi, "Optimal bi-objective redundancy allocation for systems reliability and risk management," *IEEE Trans. Cybern.*, vol. 46, no. 8, pp. 1735–1748, Aug. 2016.
[12] D. Lyu, G. Niu, E. Liu, T. Yang, G. Chen, and B. Zhang, "Uncertainty management and differential model decomposition for fault diagnosis and prognosis," *IEEE Trans. Ind. Electron.*, vol. 69, no. 5, pp. 5235–5246, May 2022.
[13] E. Zio and T. Aven, "Uncertainties in smart grids behavior and modeling: What are the risks and vulnerabilities? How to analyze them?" *Energy Policy*, vol. 39, no. 10, pp. 6308–6320, Oct. 2011.
[14] M.-X. Sun, Y.-F. Li, and E. Zio, "On the optimal redundancy allocation for multi-state series–parallel systems under epistemic uncertainty," *Rel. Eng. Syst. Saf.*, vol. 192, Dec. 2019, Art. no. 106019.
[15] Z. Chen, T. Xia, Y. Li, and E. Pan, "A hybrid prognostic method based on gated recurrent unit network and an adaptive Wiener process model considering measurement errors," *Mech. Syst. Signal Process.*, vol. 158, 2021, Art. no. 107785.
[16] H. Agarwal, J. E. Renaud, E. L. Preston, and D. Padmanabhan, "Uncertainty quantification using evidence theory in multidisciplinary design optimization," *Rel. Eng. Syst. Safety*, vol. 85, nos. 1–3, pp. 281–294, Jul./Sep. 2004.

[17] R. Ak, V. Vitelli, and E. Zio, "An interval-valued neural network approach for uncertainty quantification in short-term wind speed prediction," *IEEE Trans. Neural Netw. Learn. Syst.*, vol. 26, no. 11, pp. 2787–2800, Nov. 2015.

[18] J. Guo, Z. Wang, M. Zheng, and Y. Wang, "Uncertain multiobjective redundancy allocation problem of repairable systems based on artificial bee colony algorithm," *Chin. J. Aeronaut.*, vol. 27, no. 6, pp. 1477–1487, Dec. 2014.

[19] J. Li, B. Xin, J. Chen, and L. Wang, "S-CoEA: Subproblems co-solving evolutionary algorithm for uncertain optimization," *IEEE Trans. Cybern.*, early access, Apr. 2, 2021, doi: 10.1109/TCYB.2021.3064556.

[20] D. Gong, J. Sun, and X. Ji, "Evolutionary algorithms with preference polyhedron for interval multi-objective optimization problems," *Inf. Sci.*, vol. 233, pp. 141–161, Jun. 2013.

[21] D. Gory, X. Ji, J. Sun, and X. Sun, "Interactive evolutionary algorithms with decision-maker's preferences for solving interval multi-objective optimization problems," *Neurocomputing*, vol. 137, pp. 241–251, Aug. 2014.

[22] H. T. Nguyen, L. B. Le, and Z. Wang, "A bidding strategy for virtual power plants with the intraday demand response exchange market using the stochastic programming," *IEEE Trans. Ind. Appl.*, vol. 54, no. 4, pp. 3044–3055, Jul. 2018.

[23] A. Bozorgi-Amiri, M. S. Jabalameli, and S. M. J. M. Al-e-Hashem, "A multi-objective robust stochastic programming model for disaster relief logistics under uncertainty," *OR Spectr.*, vol. 35, no. 4, pp. 905–933, Nov. 2013.

[24] S. M. Mousavi, N. Alikar, S. T. A. Niaki, and A. Bahreininejad, "Two tuned multi-objective meta-heuristic algorithms for solving a fuzzy multi-state redundancy allocation problem under discount strategies," *Appl. Math. Model.*, vol. 39, no. 22, pp. 6968–6989, Nov. 2015.

[25] P. K. Muhuri, Z. Ashraf, and Q. M. D. Lohani, "Multiobjective reliability redundancy allocation problem with interval type-2 fuzzy uncertainty," *IEEE Trans. Fuzzy Syst.*, vol. 26, no. 3, pp. 1339–1355, Jun. 2018.

[26] M. J. Feizollahi and M. Modarres, "The robust deviation redundancy allocation problem with interval component reliabilities," *IEEE Trans. Rel.*, vol. 61, no. 4, pp. 957–965, Dec. 2012.

[27] P. Roy, B. S. Mahapatra, G. S. Mahapatra, and P. K. Roy, "Entropy based region reducing genetic algorithm for reliability redundancy allocation in interval environment," *Expert Syst. Appl.*, vol. 41, no. 14, pp. 6147–6160, Oct. 2014.

[28] E. Zhang and Q. Chen, "Multi-objective reliability redundancy allocation in an interval environment using particle swarm optimization," *Rel. Eng. Syst. Saf.*, vol. 145, pp. 83–92, Jan. 2016.

[29] D. Gong, B. Xu, Y. Zhang, Y. Guo, and S. Yang, "A similarity-based cooperative co-evolutionary algorithm for dynamic interval multiobjective optimization problems," *IEEE Trans. Evol. Comput.*, vol. 24, no. 1, pp. 142–156, Feb. 2020.

[30] J. Sun, Z. Miao, D. Gong, X. J. Zeng, and G. Wang, "Interval multi-objective optimization with memetic algorithms," *IEEE Trans. Cybern.*, vol. 50, no. 8, pp. 3444–3457, Aug. 2020.

[31] R. K. Gupta, A. K. Bhunia, and D. Roy, "A GA based penalty function technique for solving constrained redundancy allocation problem of series system with interval valued reliability of components," *J. Comput. Appl. Math.*, vol. 232, no. 2, pp. 275–284, Oct. 2009.

[32] L. Sahoo, A. K. Bhunia, and P. K. Kapur, "Genetic algorithm based multi-objective reliability optimization in interval environment," *Comput. Ind. Eng.*, vol. 62, no. 1, pp. 152–160, Feb. 2012.

[33] R. Cao, D. W. Coit, W. Hou, and Y. Yang, "Game theory based solution selection for multi-objective redundancy allocation in interval-valued problem parameters," *Rel. Eng. Syst. Saf.*, vol. 199, Jul. 2020, Art. no. 106932.

[34] C. Zhiqiang, D. Liankui, and S. Youxian, "Feasibility analysis for optimization of uncertain systems with interval parameters," *Acta Automatica Sinica*, vol. 30, no. 3, pp. 455–459, 2004.

[35] C. Jiang, X. Han, F. J. Guan, and Y. H. Li, "An uncertain structural optimization method based on nonlinear interval number programming and interval analysis method," *Eng. Struct.*, vol. 29, no. 11, pp. 3168–3177, Nov. 2007.

[36] Y. Li, P. Wang, H. B. Gooi, J. Ye, and L. Wu, "Multi-objective optimal dispatch of microgrid under uncertainties via interval optimization," *IEEE Trans. Smart Grid*, vol. 10, no. 2, pp. 2046–2058, Mar. 2019.

[37] Y. Wang, Q. Xia, and C. Kang, "Unit commitment with volatile node injections by using interval optimization," *IEEE Trans. Power Syst.*, vol. 26, no. 3, pp. 1705–1713, Aug. 2011.

[38] P. Limbourg and D. E. S. Aponte, "An optimization algorithm for imprecise multi-objective problem functions," in *Proc. IEEE Congr. Evol. Comput.*, vol. 1, Sep. 2005, pp. 459–466.

[39] D.-W. Gong, N.-n. Qin, and X.-y. Sun, "Evolutionary algorithms for multi-objective optimization problems with interval parameters," in *Proc. IEEE 5th Int. Conf. Bio-Inspired Comput., Theories Appl. (BIC-TA)*, Sep. 2010, pp. 411–420.

[40] L. Zhang *et al.*, "Cooperative artificial bee colony algorithm with multiple populations for interval multiobjective optimization problems," *IEEE Trans. Fuzzy Syst.*, vol. 27, no. 5, pp. 1052–1065, May 2019.

[41] R. Dou, C. Zong, and M. Li, "An interactive genetic algorithm with the interval arithmetic based on hesitation and its application to achieve customer collaborative product configuration design," *Appl. Soft Comput.*, pp. 384–394, 2016.

[42] H. Karshenas, C. Bielza, and P. Larrañaga, "Interval-based ranking in noisy evolutionary multi-objective optimization," *Comput. Optim. Appl.*, vol. 61, no. 2, pp. 517–555, Jun. 2015.

[43] J. Lin, M. Liu, J. Hao, and S. Jiang, "A multi-objective optimization approach for integrated production planning under interval uncertainties in the steel industry," *Comput. Oper. Res.*, vol. 72, pp. 189–203, Aug. 2016.

[44] J. Sun, D. Gong, X. Zeng, and N. Geng, "An ensemble framework for assessing solutions of interval programming problems," *Inf. Sci.*, vols. 436–437, pp. 146–161, Apr. 2018.

[45] K. Deb, A. Pratap, S. Agarwal, and T. Meyarivan, "A fast and elitist multiobjective genetic algorithm: NSGA-II," *IEEE Trans. Evol. Comput.*, vol. 6, no. 2, pp. 182–197, Aug. 2002.

[46] M. Emmerich, N. Beume, and B. Naujoks, "An EMO algorithm using the hypervolume measure as selection criterion," in *Proc. Int. Conf. Evol. Multi-Criterion Optim.* Berlin, Germany: Springer, 2005, pp. 62–76.

[47] Z. He and G. G. Yen, "Many-objective evolutionary algorithms based on coordinated selection strategy," *IEEE Trans. Evol. Comput.*, vol. 21, no. 2, pp. 220–233, Apr. 2017.

[48] Y. Xiang, Y. Zhou, M. Li, and Z. Chen, "A vector angle-based evolutionary algorithm for unconstrained many-objective optimization," *IEEE Trans. Evol. Comput.*, vol. 21, no. 1, pp. 131–152, Jul. 2016.

[49] Y. Zhou, Y. Xiang, Z. Chen, J. He, and J. Wang, "A scalar projection and angle-based evolutionary algorithm for many-objective optimization problems," *IEEE Trans. Cybern.*, vol. 49, no. 6, pp. 2073–2084, Jun. 2019.

[50] Y. Tian, R. Cheng, X. Zhang, Y. Su, and Y. Jin, "A strengthened dominance relation considering convergence and diversity for evolutionary many-objective optimization," *IEEE Trans. Evol. Comput.*, vol. 23, no. 2, pp. 331–345, Apr. 2019.

[51] C. Wang and R. Xu, "An angle based evolutionary algorithm with infeasibility information for constrained many-objective optimization," *Appl. Soft Comput.*, vol. 86, Jan. 2020, Art. no. 105911.

[52] M.-S. Chern, "On the computational complexity of reliability redundancy allocation in a series system," *Oper. Res. Lett.*, vol. 11, no. 5, pp. 309–315, 1992.

[53] M. Abouei Ardakan and A. Zeinal Hamadani, "Reliability–redundancy allocation problem with cold-standby redundancy strategy," *Simul. Model. Pract. Theory*, vol. 42, pp. 107–118, Mar. 2014.

[54] A. K. Bhunia, L. Sahoo, and D. Roy, "Reliability stochastic optimization for a series system with interval component reliability via genetic algorithm," *Appl. Math. Comput.*, vol. 216, no. 3, pp. 929–939, Apr. 2010.

[55] A. Sengupta, T. K. Pal, and D. Chakraborty, "Interpretation of inequality constraints involving interval coefficients and a solution to interval linear programming," *Fuzzy Sets Syst.*, vol. 119, no. 1, pp. 129–138, Apr. 2001.

[56] A. Sengupta and T. K. Pal, "On comparing interval numbers," *Eur. J. Oper. Res.*, vol. 127, no. 1, pp. 28–43, Nov. 2000.

[57] C.-M. Lai and W.-C. Yeh, "Two-stage simplified swarm optimization for the redundancy allocation problem in a multi-state bridge system," *Rel. Eng. Syst. Saf.*, vol. 156, pp. 148–158, Dec. 2016.

[58] Y. Wang and L. Li, "A PSO algorithm for constrained redundancy allocation in multi-state systems with bridge topology," *Comput. Ind. Eng.*, vol. 68, pp. 13–22, Feb. 2014.

[59] J. Zou, Q. Li, S. Yang, H. Bai, and J. Zheng, "A prediction strategy based on center points and knee points for evolutionary dynamic multi-objective optimization," *Appl. Soft Comput.*, vol. 61, pp. 806–818, Dec. 2017.

[60] X. Zhang, Y. Tian, and Y. Jin, "A knee point-driven evolutionary algorithm for many-objective optimization," *IEEE Trans. Evol. Comput.*, vol. 19, no. 6, pp. 761–776, Dec. 2015.

[61] I. Das, "On characterizing the 'knee' of the Pareto curve based on normal-boundary intersection," *Structural Optim.*, vol. 18, nos. 2–3, pp. 107–115, 1999.
[62] M. T. Jensen, "Reducing the run-time complexity of multiobjective EAs: The NSGA-II and other algorithms," *IEEE Trans. Evol. Comput.*, vol. 7, no. 5, pp. 503–515, Oct. 2003.
[63] E. Zitzler and L. Thiele, "Multiobjective evolutionary algorithms: A comparative case study and the strength Pareto approach," *IEEE Trans. Evol. Comput.*, vol. 3, no. 4, pp. 257–271, Nov. 1999.
[64] G. Minella, R. Ruiz, and M. Ciavotta, "Restarted iterated Pareto greedy algorithm for multi-objective flowshop scheduling problems," *Comput. Oper. Res.*, vol. 38, no. 11, pp. 1521–1533, Nov. 2011.
[65] Q. Zhang, S. Yang, M. Liu, J. Liu, and L. Jiang, "A new crossover mechanism for genetic algorithms for Steiner tree optimization," *IEEE Trans. Cybern.*, early access, Jul 31, 2020, doi: 10.1109/TCYB.2020.3005047.

Yue Xu received the B.Eng. degree in software engineering from Xidian University, Xi'an, in 2016. She is currently pursuing the Ph.D. degree in computer science and technology with the Nanjing University of Aeronautics and Astronautics, Nanjing, China. Her current research interests include reliability design, intelligent optimization methods, and deep reinforcement learning.

Dechang Pi is currently a Full Professor with the Nanjing University of Aeronautics and Astronautics. He has completed over 20 scientific research projects and published more than 100 papers and ten invention patents. In the past 20 years, he has been engaged in the research about intelligent data analysis, data-driven reliability analysis, and their application. He was awarded four times by the Ministry of Industry and the Informationization of China.

Shengxiang Yang (Senior Member, IEEE) received the Ph.D. degree from Northeastern University, Shenyang, China, in 1999. He is currently a Professor of computational intelligence and the Deputy Director of the Institute of Artificial Intelligence, School of Computer Science and Informatics, De Montfort University, Leicester, U.K. He has over 350 publications with an H-index of 62 according to Google Scholar. His current research interests include evolutionary computation, swarm intelligence, artificial neural networks, data mining and data stream mining, and relevant real-world applications. He serves as an Associate Editor/Editorial Board Member for a number of international journals, such as the IEEE TRANSACTIONS ON EVOLUTIONARY COMPUTATION, IEEE TRANSACTIONS ON CYBERNETICS, *Information Sciences*, and *Enterprise Information Systems*.

Yang Chen is currently pursuing the Ph.D. degree with the College of Computer Science and Technology, Nanjing University of Aeronautics and Astronautics. His research interests include swarm intelligence optimization technology, UAV path planning, and edge computing.

Shuo Qin received the B.Eng. and M.Eng. degrees in software engineering from the Lanzhou University of Technology University, Lanzhou, in 2016 and 2019, respectively. He is currently pursuing the Ph.D. degree in computer science and technology with the Nanjing University of Aeronautics and Astronautics, Nanjing, China. His current research interests include cloud computing, intelligent optimization methods, and object detection.

Enrico Zio (Senior Member, IEEE) received the B.Sc. degree in nuclear engineering from the Politecnico di Milano, Milan, Italy, in 1991, the M.Sc. degree in mechanical engineering from the University of California at Los Angeles (UCLA), Los Angeles, CA, USA, in 1995, the Ph.D. degree in nuclear engineering from the Politecnico di Milano in 1996, and the Ph.D. degree in probabilistic risk assessment from the Massachusetts Institute of Technology (MIT), Cambridge, MA, USA, in 1998. He is currently a Full Professor with the Centre for Research on Risk and Crises of Ecole de Mines, ParisTech, PSL Research University, Paris, France; a Full Professor and the President of the Alumni Association, Politecnico di Milano; an Eminent Scholar with Kyung Hee University, Seoul, South Korea; a Distinguished Guest Professor with Tsinghua University, Beijing, China. He is also an Adjunct Professor with the City University of Hong Kong, Hong Kong; Beihang University, Beijing; and Wuhan University, Wuhan, China. He is the Co-Director of the Center for Reliability and Safety of Critical Infrastructures and the Sino-French Laboratory of Risk Science and Engineering, Beihang University. His research interests include the modeling of the failure-repair-maintenance behavior of components and complex systems, for the analysis of their reliability, maintainability, prognostics, safety, vulnerability, resilience, and security characteristics, and on the development and use of Monte Carlo simulation methods, artificial techniques, and optimization heuristics.